Mem. S.A.It. Vol. 80, 658

Memorie della

Cloud formation and dynamics in cool dwarf and hot exoplanetary atmospheres

Adam J. Burgasser

Center of Astrophysics and Space Sciences, University of California, 9500 Gilman Dr., San Diego, CA 92093, USA, e-mail: aburgasser@ucsd.edu

Abstract. The lowest-mass stars, brown dwarfs and extrasolar planets present challenges and opportunities for understanding dynamics and cloud formation processes in low-temperature atmospheres. For brown dwarfs, the formation, variation and rapid depletion of photospheric clouds in L- and T-type dwarfs, and spectroscopic evidence for non-equilibrium chemistry associated with vertical mixing, all point to a fundamental role for dynamics in vertical abundance distributions and cloud/grain formation cycles. For exoplanets, azimuthal heat variations and the detection of stratospheric and exospheric layers indicate multi-layered, asymmetric atmospheres that may also be time-variable (particularly for systems with highly elliptical orbits). Dust and clouds may also play an important role in the thermal energy balance of exoplanets through albedo effects. For all of these cases, 3D atmosphere models are becoming an increasingly essential tool for understanding spectral and temporal properties. In this review, I summarize the observational evidence for clouds and dynamics in cool dwarf and hot exoplanetary atmospheres, outstanding problems associated with these processes, and areas where effective synergy can be achieved.

Key words. Stars: atmospheres – Stars: fundamental parameters – Stars: low-mass, brown dwarfs – Extrasolar planets

1. Introduction

Fifteen years ago, the first examples of brown dwarfs and extrasolar planets were discovered, sources which continue to challenge our understanding of low temperature atmospheres. Several hundred very low-mass stars and brown dwarfs are now known (the latter distinguished by their lack of core hydrogen fusion), encompassing two newly defined spectral classes, the L dwarfs and the T dwarfs (see review by Kirkpatrick 2005). Roughly 300 extrasolar planets have been found through Doppler shift, transit, microlensing and direct detection techniques. Collectively, these low-temperature sources span a broad range of mass (1 $M_{Jupiter} \lesssim M \lesssim 100\ M_{Jupiter}$), photospheric temperature (100 K $\lesssim T \lesssim$ 2500 K), surface gravity ($3 \lesssim \log g \lesssim 5.5$ cm s^{-2}), age (few Myr to few Gyr), elemental composition, rotation period (hours to days), magnetic activity, degree of external heating and interior structure. Yet all are related by their cool, molecule-rich, dynamic atmospheres.

While direct studies of cool dwarf atmospheres have been feasible since their discovery, it is only recently that techniques to probe exoplanet atmospheres have been realized. The best-constrained exoplanets are

Send offprint requests to: A. J. Burgasser those which closely orbit and transit their host stars—so-called "Hot Jupiters"—allowing reflectance and thermal spectrophotometry during secondary transit (e.g., Charbonneau et al. 2005; Deming et al. 2005), and transmission spectrophotometry during primary transit (e.g., Charbonneau et al. 2002). Phase curves for non-transiting systems have also been measured (e.g., Harrington et al. 2006), and the recent direct detection of planets around the young stars Fomalhaut, β Pictoris and HR 8799 (Kalas et al. 2008; Marois et al. 2008; Lagrange et al. 2009) through high contrast imaging techniques have opened the door to direct investigations of exoplanet atmospheres.

Two themes are prominent in the interpretation of observational data for low-temperature stellar, brown dwarf and exoplanetary atmospheres: clouds and dynamics. Condensate clouds are an important source of opacity and a component in the chemical network; they also modulate the albedos, energy budgets and atmospheric structure of exoplanets under intense irradiation. Dynamics are responsible for the redistribution of heat and modification of chemical abundances, and are likely fundamental to cloud formation and evolution processes.

In this review, I summarize our current observational evidence for clouds and dynamics in cool dwarfs and hot exoplanets, and note outstanding issues in their role in emergent spectral energy distributions, long-term thermal evolution, albedo, and temporal and azimuthal variability. I conclude with a discussion of opportunities for synergy in future generations of cool dwarf and exoplanet models, with a view toward 3D simulations.

2. Clouds and dynamics in cool dwarf atmospheres

2.1. Observational evidence for condensate clouds

The atmospheres of the lowest-temperature dwarfs are rich in molecular gas species and neutral metal elements, which produce useful spectral discriminants for bulk properties such as effective temperature ($T_{\rm eff}$), surface gravity, and metallicity. Importantly, the $T_{\rm eff}$s of L dwarfs (1400 K $\lesssim T_{\rm eff} \lesssim$ 2300 K; Golimowski et al. 2004) span the gas/liquid and gas/solid phase transitions for a number of refractory species, including iron, silicates, titanates, and other metal oxides (Lodders 2002). Evidence for these species in L dwarf photospheres has been inferred from their very red near-infrared colors (thermal emission from hot dust); muted H_2O steam bands (the result of condensate opacity at flux peaks); and depletion of gaseous precursors to condensates such as TiO and VO (e.g., Burrows & Sharp 1999; Allard et al. 2001). More recently, the *Spitzer Space Telescope* has directly detected silicate grain absorption at mid-infrared wavelengths (Figure 1; Cushing et al. 2006). These observations make clear the prominent role of condensates in L dwarf atmospheres.

Conversely, the T dwarfs, which comprise a cooler, later stage of evolution for brown dwarfs (600 K $\lesssim T_{\rm eff} \lesssim$ 1400 K), exhibit relatively condensate-free photospheres as evident from their blue near-infrared colors and prominent molecular gas bands. Strong features from neutral alkalis, whose pressure-broadened wings absorb much of the 0.5–1.0 μm light in T dwarf spectra, also indicate that condensates have been cleared out of the photosphere. These species should be depleted into feldspars in the presence of silicates; their presence requires the sequestration of condensates to deeper levels[1] (Burrows et al. 2000).

The development of 1D condensate cloud models (e.g., Ackerman & Marley 2001) has resolved many of these issues, although not all (§ 2.3). Rather than being fully mixed in the atmosphere, clouds of condensate species are constrained between a phase transition layer and a cloud top set by a balance of gravitational settling and mixing (the latter can be parameterized by a "settling efficiency" or "cloud top temperature"). For the L dwarfs, these cloud layers reside at the photosphere, so their influence on the spectral energy distribution is pronounced. For the T dwarfs, the cloud lay-

[1] A similar effect explains GeH_4 abundances in the atmosphere of Jupiter (Fegley & Lodders 1994).

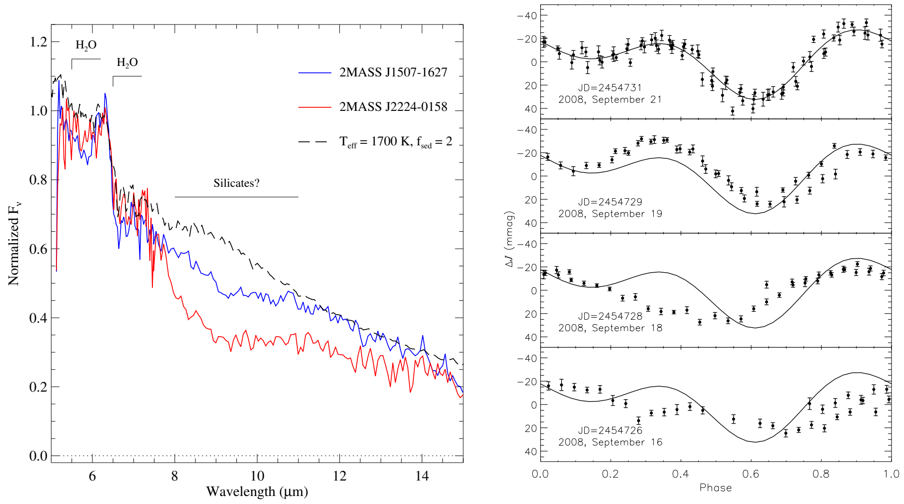

Fig. 1. (Left) Silicate grain absorption in the mid-infrared spectra of two equivalently-classified L dwarfs (solid lines) compared to a cloud model from M. Marley and collaborators (dashed line). The L dwarf spectra also illustrate variations in the strength of this feature that correlate with near-infrared color (from Burgasser et al. 2008). (Right) J-band light curve for the T2.5 SIMP 0136 phased to a 2.4 hr period, showing variation in both amplitude and phase over the course of 5 days (solid lines are a fit to data from 2008 September 21). Such light curve evolution suggest a dynamic cloud layer (from Artigau et al. 2009)

ers have sunk below the photosphere, so that the emergent spectral energy distribution is largely "condensate-free". It is important to note that the various condensates, while condensing at different temperatures, are probably well-mixed by convection and turbulent gas motion (e.g., Burrows et al. 2006). This raises the possibility of fairly complex grain chemistry, including nonequilibrium hybrid grain formation (e.g., Helling et al. 2008).

Observational evidence supporting the presence of condensate clouds is also found in large source-to-source near-infrared color variations among equivalently-classified L dwarfs, at wavelengths where cloud opacity is most prominent (e.g., Knapp et al. 2004). Early evidence suggests that near-infrared color is correlated with the 9 μm silicate grain feature (Figure 1; Burgasser et al. 2008). In addition, temporal variability, both photometric and spectroscopic, has been observed in several low-temperature dwarfs (see review by Goldman 2005), most importantly those whose atmospheres are too neutral to couple with magnetic fields and form spots (e.g., Mohanty et al. 2002). The variability likely arises from rotational modulation of surface asymmetries in global cloud coverage, since light curve periods are generally consistent with rotational line broadening (e.g., Reiners & Basri 2008). Variability amplitudes are typically <5%, on par with amplitudes in Jupiter's optical light curve (although the 5 μm variations on Jupiter are closer to 20%; Gelino & Marley 2000). In addition, the rapid rotations of low-mass dwarfs ($V_{\rm rot} \sim 30$ kms^{-1}) and their high surface gravities ($\log g \sim 5$ cgs) translate into characteristic Rhines lengths—an estimate of jet band width—and Rossby deformation radii—an estimate of vorticity scale—that are similar to Jupiter and Saturn.[2]

[2] The Rhines length is $(RU/2\Omega\cos\phi)^{1/2}$, where R is the radius of the body, U the characteristic wind speed, Ω the rotation angular rate and ϕ the latitude. Assuming $U \sim 1$ kms^{-1} (of order the sound speed) and $2R\Omega\cos\phi \sim V_{rot} \sim$ 30 kms^{-1} (e.g., Reiners & Basri 2008) yields a length scale of ~0.2R. The Rossby deformation

Notably, photometric light curves are observed to evolve over time, both in amplitude and phase, occasionally disappearing altogether (Figure 1). This is an indication of surface cloud evolution over daily- to yearly-timescales.

2.2. Observational evidence for dynamics

Photometric variability and variance suggest that atmospheric dynamics is an important contributor to cloud formation and evolution. More direct evidence comes from the nonequilibrium chemical abundances of CO, CH_4 and NH_3 observed in T dwarf spectra. The conversion of the carbon reservoir from CO to CH_4 signals the transition between the L dwarf and T dwarf classes, and in chemical equilibrium this is largely complete by $T_{\rm eff} \approx 1000$ K (e.g., Burrows & Sharp 1999). However, CO absorption is seen to persist well into the T dwarf regime, substantially in excess (>1000×) of chemical equilibrium calculations (e.g., Noll et al. 1997). Nitrogen chemistry—the conversion of N_2 to NH_3 at $T_{\rm eff} \approx 700$ K—is similarly in disequilibrium, with the latter molecule found to be significantly underabundant (Figure 2; Saumon et al. 2006).

The nonequilibrium abundances of these species can be explained by the presence of vertical mixing in the photosphere (Griffith & Yelle 1999). Both CO and N_2 are strongly bonded diatomic molecules, and their conversion to CH_4 and NH_3 can occur over longer timescales than those vertical mixing ($\tau_{\rm mix}$). As a result, CO and N_2 are found in cooler regions with abundances in excess of thermal equilibrium; equivalently, their products CH_4 and NH_3 are underabundant. Current studies parameterize the mixing timescale with an eddy diffusion coefficient, $\tau_{\rm mix} \approx H^2/{\rm K}_{\rm zz}$, where H is the atmospheric scaleheight (Griffith & Yelle 1999). Observed CO overabundances and NH_3 underabundances can be reproduced with diffusion coefficients of order 10^2–10^6 cm^2 s^{-1} (e.g., (Saumon et al. 2007)). These values are well below full convection, but are nevertheless indicative with vigorous mixing in the photosphere. Importantly, mixing appears to be a universal property of L and T dwarf atmospheres (Stephens et al. 2009).

radius is $NH/2\Omega \sin\phi$, where N is the Brunt-Väisälä frequency (vertical oscillation of displaced air parcels) and H the scale height. Estimating the former as $\sqrt{g/H}$, with $g \approx 10^5$ cm s^{-2} and $H \approx 1$ km (Griffith & Yelle 1999), and $2R\Omega \sin\phi \sim V_{rot} \sim 30$ kms^{-1} yields a scale of $0.03R$. For Jupiter and Saturn, these scales are $0.14R$ and $0.03R$ (Showman et al. 2008).

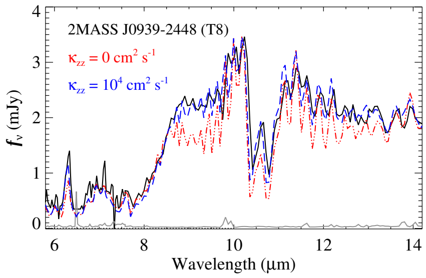

Fig. 2. Mid-infrared spectrum of the late-type T dwarf 2MASS J0939-2448 (black line) compared to $T_{\rm eff}$ = 600 K, $\log g$ = 5 cm s^{-2} atmosphere models from Saumon et al. (2007) incorporating equilibrium chemistry (red dot-dashed line) and vertical mixing (blue dashed line). Mixing is consistently required to match attenuated absorption bands of NH_3 in the 9–11 μm region of T dwarf spectra, as well as enhanced CO absorption in the 4.5–5 μm region.

2.3. Dynamics and cloud evolution at the L dwarf/T dwarf transition

Current 1D cloud models have proven successful in providing a conceptual understanding of how condensates, prominent in L dwarf photospheres, are largely absent in T dwarf photospheres. However these models have difficulty reproducing two outstanding features of this transition: substantial evolution in spectral energy distributions over narrow temperature ($\Delta T_{\rm eff} \approx 200$–400 K) and luminosity scales ($\Delta \log {\rm L}/{\rm L}_{\rm bol} \approx 0.3$ dex; e.g., Golimowski et al. 2004), and a dramatic increase in 1 μm surface brightnesses (the "J-band bump"; e.g., Tinney et al. 2003). Importantly, the latter ef-

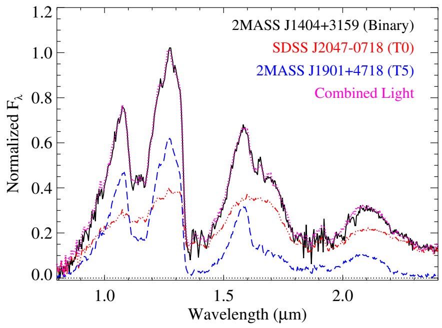

Fig. 3. Spectral decomposition of the resolved T0 + T5 binary 2MASS J1404-3159 (Looper et al. 2008), illustrating the J-band bump across the L dwarf/T dwarf transition. Spectral templates scaled to match resolved photometry and combined light spectroscopy (black line) indicate a secondary (blue dashed line) that is ~50% brighter than its primary (red dot-dashed line) at the 1.05 and 1.25 μm flux peaks. These wavelengths are dominated by condensate cloud opacity in the L dwarfs.

fect has been observed in the components of L dwarf/T dwarf binaries, indicating that age, surface gravity or composition variations are not responsible (Fig. 3; Burgasser et al. 2006; Liu et al. 2006.)

These surprising trends suggest a relatively rapid dissolution of condensate clouds at the L dwarf/T dwarf transition. The 1.05 and 1.25 μm spectral peaks, minima in molecular gas opacity, are dominated by condensate opacity in the L dwarfs. A brightening in this region would be expected if the condensates were suddenly removed (a deepening of alkali lines and FeH absorption at these flux peaks are also seen across this transition). But what removes the clouds? Ackerman & Marley (2001) and Burgasser et al. (2002) have proposed a progressive fragmentation of the cloud layer, revealing hot spots similar to those observed on Jupiter and Saturn at 5 μm; Knapp et al. (2004) have proposed a global increase in condensate sedimentation efficiency. Interestingly, atmospheric models by Burrows et al. (2006) predict the formation of a detached convective region in the photospheres of L dwarfs triggered by dust opacity, which merges with the lower convective boundary around the L dwarf/T dwarf transition. What role this transition has on cloud structure will require more detailed 3D atmosphere modeling to simultaneously explore dynamics and cloud formation (see contribution by B. Freytag).

3. Clouds and dynamics in exoplanet atmospheres

3.1. Empirical constaints on cloud properties

Like the L dwarfs, exoplanets orbiting close to solar-type stars have equilibrium temperatures ($T_{\rm eq}$) spanning phase transitions for several refractory species. Hence, these objects are also expected to host dusty atmospheres. Yet observational evidence remains ambiguous. Transmission spectroscopy has revealed muted atomic and molecular features in some sources (e.g., Charbonneau et al. 2002; Pont et al. 2008) which, like the H_2O bands in L dwarf spectra, may be attributable to obscuring condensate (haze) opacity. In addition, Richardson et al. (2007) have claimed the detection of silicate emission from HD 20948b, albeit at low significance. These results stand in contrast to the very low albedo of planets such as HD 20948b, A_g<0.08 compared to Jupiter's A_g≈0.5 (Rowe et al. 2008). Burrows et al. (2008) have found such albedos consistent with a condensate-free atmosphere. On the other hand, Fortney (2005) have proposed that the slant angle observations that characterize transit spectroscopy can result in a 1-2 order of magnitude increase in condensate and haze optical depth, allowing a thin condensate layer with little effect on reflectance to absorb strongly in transmission. Since other processes, such as ionization from stellar irradiation or absorption from stratospheric gas (§ 3.4) can also mute photospheric molecular absorption in transmission, the presence and characteristics of condensates in exoplanets remain open questions.

3.2. Variability

As with cool dwarfs, variability in exoplanets could support the presence of clouds, particularly in repeated observations of the same longitude (i.e., multiple measurements at a particular phase). However, while a few studies have suggested the presence of orbit-to-orbit variability in well-studied exoplanets (e.g., Madhusudhan & Seager 2009), existing datasets remain too limited in temporal coverage to make definitive claims (long-term warm *Spitzer* programs are likely to improve this situation). Dramatic variations in cloud coverage are unlikely, as the typical Rhines lengths and Rossby deformation radii of slowly-rotating, tidally-locked exoplanets are of order the planetary radius (Showman et al. 2008). This is the case of circularized planets; eccentric planets, on the other hand, can have dramatic temporal variations in the course of single orbit. An extreme example is the highly eccentric (e = 0.93) transitting exoplanet HD 80606b, whose brightness temperature was observed to increase by ~700 K over a 6 hr period near periastron (Laughlin et al. 2009). This system undergoes dramatic changes in irradiation over its 0.3 yr orbit—a factor of over 800 between its 0.03 AU periastron and 0.87 AU apastron—so interorbit variability in its atmospheric properties are almost certain.

3.3. Dynamics driven by irradiation

Thermal imaging of some exoplanet atmospheres over significant fractions of their orbits reveal two features indicative of dynamics: thermal peaks offset by 10–30° from the substellar longitude and small variations between dayside and nightside brightness temperatures (Figure 4; e.g., Knutson et al. 2009). Both indicate the presence of winds and jets circulating heat around the planet. Advanced hydrodynamic models generally confirm these results, although not necessarily the phase amplitudes (e.g., Langton & Laughlin 2007; Showman et al. 2009). Such behavior is not universal; some exoplanets exhibit large day-night flux variations indicative of minimal heat circulation (e.g., Harrington et al. 2006).

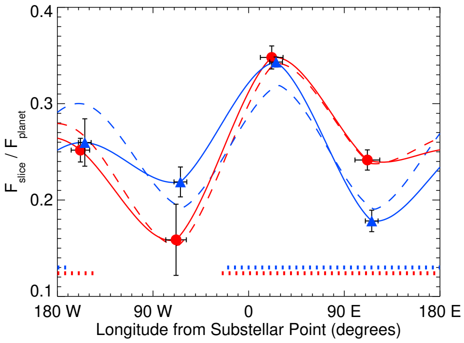

Fig. 4. Longitudinal surface brightness as a percentage of total surface flux for the transitting exoplanet HD 189733b at 8 μm (blue triangles) and 24 μm (red circles). The brightness peak at both wavelengths is offset from the substellar point by ~20°, indicating strong horizontal flows. The relatively modest variation between dayside and nightside flux indicates heat convection around the planet (from Knutson et al. 2009).

In such cases, azimuthal heat gradients will induce azimuthal chemical gradients, likely modulated by the same nonequilibrium chemistry present in brown dwarf atmospheres (e.g., Cooper & Showman 2006).

3.4. Stratospheres and exospheres

Molecular *emission* has been detected during the secondary transit of a handful of exoplanets (e.g., Knutson et al. 2008), indicating the occasional presence of an upper atmosphere temperature inversion, or stratosphere (Figure 5; Fortney et al. 2006; Burrows et al. 2007). Stratospheres appear to be particularly common in highly irradiated planets (highest $T_{\rm eq}$) and can arise if efficient optical/UV absorbers are present high in the atmosphere. Primary candidates for these absorbers are currently TiO and VO, although Spiegel et al. (2009) have pointed out that TiO gas requires significant vertical mixing across the condensation cold trap, with eddy coefficients of K_{zz} $\gtrsim 10^7$ cm^2 s^{-1}. This is somewhat more vigorous than the mixing inferred in brown dwarf atmospheres (§ 2.2), butit could be powered by intense stellar irradiation. The presence of a

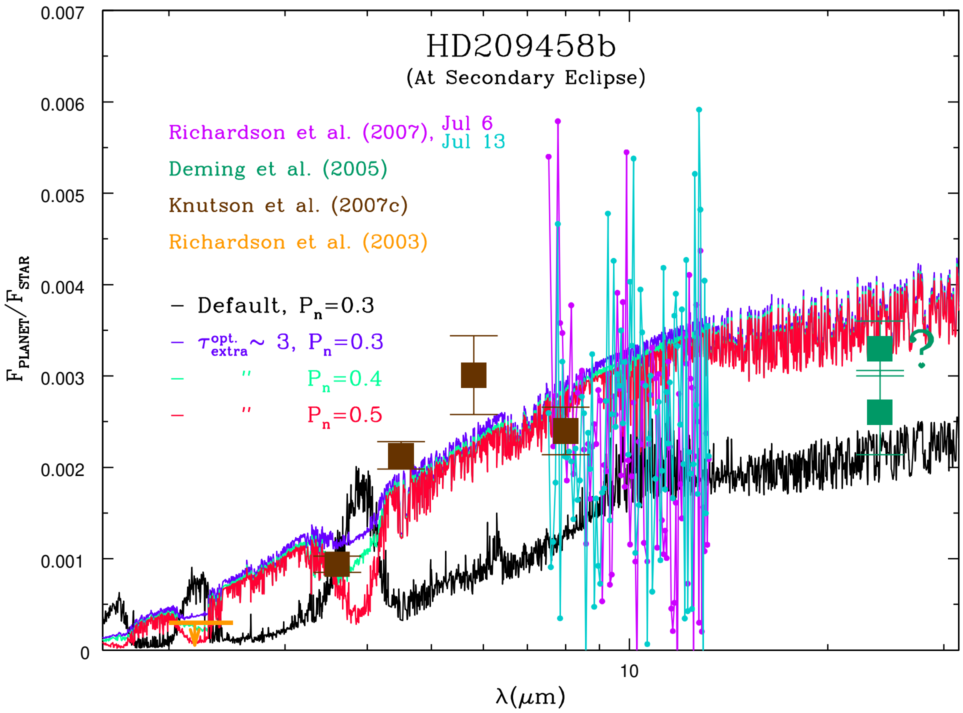

Fig. 5. Planet-to-star flux during secondary transit for HD 209458b. Mid-infrared measurements (squares and points with error bars) are compared to models with (purple, green and red lines) and without (black line) the addition of stratospheric opacity. Photometry over 4–7 μm from Knutson et al. (2008, labeled 2007c) can only be reproduced with the inclusion of this opacity (Burrows et al. 2007).

stratosphere modifies the energy budget, pressure/temperature profile, chemical distribution and emergent spectral flux of an exoplanet, and has been proposed as a natural division between hot exoplanet types (e.g., Fortney et al. 2008).

More controversial is the possible detection of exospheres around exoplanets, atmospheric material blown off by high levels of UV irradiation. Vidal-Madjar et al. (2003) first reported this effect in HD 209485b on the basis of deep Lyα hydrogen absorption during primary eclipse (or more accurately, a large absorption cross-section). Several models have validated this observation (e.g,. Lammer et al. 2003), although Ben-Jaffel (2007) claim the evaporation detection to be spurious (however, Vidal-Madjar et al. 2008 refute this). The estimated evaporation rate of material off HD 209458b has been estimated to be as high as 0.1 $M_{Jupiter}$ Gyr^{-1}, a value that may be uniquely high given the equivalent mass distributions of exoplanets at close and far separations (Hubbard et al. 2007). Since this process has profound implications on the frequency of Hot Jupiters (which might otherwise be evaporated away), further study is warranted.

4. Opportunities for synergy

The similar properties of cool dwarf and hot exoplanet atmospheres (low temperatures, molecule-rich atmospheres, presence of clouds and dynamics) but distinct approaches to their study (e.g, direct observations versus transit detection and phase variation) indicate opportunities for synergistic efforts in addressing common, outstanding problems. These include the detailed microphysics of condensate grains (size distribution, composition, spectral properties), the temporal behavior of clouds, the influence of vertical and azimuthal mixing on chemical abundances, the formation of jets and vorticities, and the opacities of major molecular species. Some of these efforts are better addressed in cool dwarf studies, due to the ease of detailed, direct observation; others will benefit from the well-characterized bulk properties (mass and radius) and surface mapping achievable with transiting exoplanets. As advances are made in detailed, 3D modeling of low-temperature atmospheres and associated processes, this author encourages the use of both cool dwarf and hot exoplanet observations as empirical testbeds.

Acknowledgements. The author acknowledges helpful comments from J. Fortney, N. Madhusudhan and D. Saumon in the preparation of this review, and thanks E. Artigau, A. Burrows and H. Knutson for electronic versions of their published figures and permission to reproduce them here.

References

Ackerman, A. S. & Marley, M. S. 2001, ApJ, 556, 872

Allard, F., Hauschildt, P. H., Alexander, D. R., Tamanai, A., & Schweitzer, A. 2001, ApJ, 556, 357

Artigau, É., Bouchard, S., Doyon, R., & Lafrenière, D. 2009, ApJ, 701, 1534

Ben-Jaffel, L. 2007, ApJ, 671, L61

Burgasser, A. J., Kirkpatrick, J. D., Cruz, K. L., et al. 2006, ApJS, 166, 585

Burgasser, A. J., Looper, D. L., Kirkpatrick, J. D., Cruz, K. L., & Swift, B. J. 2008, ApJ, 674, 451

Burgasser, A. J., Marley, M. S., Ackerman, A. S., et al. 2002, ApJ, 571, L151

Burrows, A., Hubeny, I., Budaj, J., Knutson, H. A., & Charbonneau, D. 2007, ApJ, 668, L171

Burrows, A., Ibgui, L., & Hubeny, I. 2008, ApJ, 682, 1277

Burrows, A., Marley, M. S., & Sharp, C. M. 2000, ApJ, 531, 438

Burrows, A. & Sharp, C. M. 1999, ApJ, 512, 843

Burrows, A., Sudarsky, D., & Hubeny, I. 2006, ApJ, 640, 1063

Charbonneau, D., Allen, L. E., Megeath, S. T., et al. 2005, ApJ, 626, 523

Charbonneau, D., Brown, T. M., Noyes, R. W., & Gilliland, R. L. 2002, ApJ, 568, 377

Cooper, C. S. & Showman, A. P. 2006, ApJ, 649, 1048

Cushing, M. C. et al. 2006, ApJ, 648, 614

Deming, D., Seager, S., Richardson, L. J., & Harrington, J. 2005, Nature, 434, 740

Fegley, B. J. & Lodders, K. 1994, Icarus, 110, 117

Fortney, J. J. 2005, MNRAS, 364, 649

Fortney, J. J., Lodders, K., Marley, M. S., & Freedman, R. S. 2008, ApJ, 678, 1419

Fortney, J. J., Saumon, D., Marley, M. S., Lodders, K., & Freedman, R. S. 2006, ApJ, 642, 495

Gelino, C. & Marley, M. 2000, in Astronomical Society of the Pacific Conference Series, Vol. 212, From Giant Planets to Cool Stars, ed. C. A. Griffith & M. S. Marley, 322–+

Goldman, B. 2005, Astronomische Nachrichten, 326, 1059

Golimowski, D. A. et al. 2004, AJ, 127, 3516

Griffith, C. A. & Yelle, R. V. 1999, ApJ, 519, L85

Harrington, J., Hansen, B. M., Luszcz, S. H., et al. 2006, Science, 314, 623

Helling, C., Dehn, M., Woitke, P., & Hauschildt, P. H. 2008, ApJ, 675, L105

Hubbard, W. B., Hattori, M. F., Burrows, A., & Hubeny, I. 2007, ApJ, 658, L59

Kalas, P., Graham, J. R., Chiang, E., et al. 2008, Science, 322, 1345

Kirkpatrick, J. D. 2005, ARA&A, 43, 195

Knapp, G. R. et al. 2004, AJ, 127, 3553

Knutson, H. A., Charbonneau, D., Allen, L. E., Burrows, A., & Megeath, S. T. 2008, ApJ, 673, 526

Knutson, H. A., Charbonneau, D., Cowan, N. B., et al. 2009, ApJ, 690, 822

Lagrange, A.-M., Gratadour, D., Chauvin, G., et al. 2009, A&A, 493, L21

Lammer, H., Selsis, F., Ribas, I., et al. 2003, ApJ, 598, L121

Langton, J. & Laughlin, G. 2007, ApJ, 657, L113
Laughlin, G., Deming, D., Langton, J., et al. 2009, Nature, 457, 562
Liu, M. C., Leggett, S. K., Golimowski, D. A., et al. 2006, ApJ, 647, 1393
Lodders, K. 2002, ApJ, 577, 974
Looper, D. L., Gelino, C. R., Burgasser, A. J., & Kirkpatrick, J. D. 2008, ApJ, 685, 1183
Madhusudhan, N. & Seager, S. 2009, ApJ, submitted
Marois, C., Macintosh, B., Barman, T., et al. 2008, Science, 322, 1348
Mohanty, S., Basri, G., Shu, F., Allard, F., & Chabrier, G. 2002, ApJ, 571, 469
Noll, K. S., Geballe, T. R., & Marley, M. S. 1997, ApJ, 489, L87+
Pont, F., Knutson, H., Gilliland, R. L., Moutou, C. & Charbonneau, D. 2008, MNRAS, 385, 109
Reiners, A. & Basri, G. 2008, ApJ, 684, 1390
Richardson, L. J., Deming, D., Horning, K., Seager, S., & Harrington, J. 2007, Nature, 445, 892
Rowe, J. F., Matthews, J. M., Seager, S., et al. 2008, ApJ, 689, 1345
Saumon, D., Marley, M. S., Cushing, M. C., et al. 2006, ApJ, 647, 552
Saumon, D., Marley, M. S., Leggett, S. K., et al. 2007, ApJ, 656, 1136
Showman, A. P., Fortney, J. J., Lian, Y., et al. 2009, ApJ, 699, 564
Showman, A. P., Menou, K., & Cho, J. Y.-K. 2008, in Astronomical Society of the Pacific Conference Series, Vol. 398, Astronomical Society of the Pacific Conference Series, ed. D. Fischer, F. A. Rasio, S. E. Thorsett, & A. Wolszczan, 419–+
Spiegel, D. S., Silverio, K., & Burrows, A. 2009, ApJ, 699, 1487
Stephens, D. C., Leggett, S. K., Cushing, M. C., et al. 2009, ApJ, 702, 154
Tinney, C. G., Burgasser, A. J., & Kirkpatrick, J. D. 2003, AJ, 126, 975
Vidal-Madjar, A., Lecavelier des Etangs, A., Désert, J.-M., et al. 2003, Nature, 422, 143
Vidal-Madjar, A., Lecavelier des Etangs, A., Désert, J.-M., et al. 2008, ApJ, 676, L57